RESEARCH ARTICLE OPEN ACCESS

A 3′UTR Insertion Is a Candidate Causal Variant at the *TMEM106B* Locus Associated With Increased Risk for FTLD-TDP

Augustine Chemparathy, MS,* Yann Le Guen, PhD,* Yi Zeng, PhD, John Gorzynski, DVM, PhD, Tanner D. Jensen, BS, Chengran Yang, PhD, Nandita Kasireddy, BA, Lia Talozzi, PhD, Michael Belloy, PhD, Ilaria Stewart, BA, Aaron D. Gitler, PhD, Anthony D. Wagner, PhD, Elizabeth Mormino, PhD, Victor W. Henderson, MD, MS, Tony Wyss-Coray, PhD, Euan Ashley, MB, ChB, DPhil, Carlos Cruchaga, PhD,† and Michael D. Greicius, MD, MPH†

Correspondence
Dr. Greicius
greicius@stanford.edu

Neurol Genet 2024;10:e200124. doi:10.1212/NXG.0000000000200124

Abstract

Background and Objectives

Single-nucleotide variants near *TMEM106B* associate with the risk of frontotemporal lobar dementia with TDP-43 inclusions (FTLD-TDP) and Alzheimer disease (AD) in genome-wide association studies (GWASs), but the causal variant at this locus remains unclear. Here, we asked whether a novel structural variant on *TMEM106B* is the causal variant.

Methods

An exploratory analysis identified structural variants on neurodegeneration-related genes. Subsequent analyses focused on an *Alu* element insertion on the 3′UTR of *TMEM106B*. This study included data from longitudinal aging and neurogenerative disease cohorts at Stanford University, case-control cohorts in the Alzheimer Disease Sequencing Project (ADSP), and expression and proteomics data from Washington University in St. Louis (WUSTL). Four hundred thirty-two individuals from 2 Stanford aging cohorts were whole-genome long-read and short-read sequenced. A total of 16,906 samples from ADSP were short-read sequenced. Genotypes, transcriptomics, and proteomics data were available in 1,979 participants from an aging and dementia cohort at WUSTL. Selection criteria were specific to each cohort. In primary analyses, the linkage disequilibrium between the *TMEM106B* locus variants in the FTLD-TDP GWAS and the 3′UTR insertion was estimated. We then estimated linkage by ancestry in the ADSP and evaluated the effect of the *TMEM106B* lead variant on mRNA and protein levels.

Results

The primary analysis included 432 participants (52.5% female, age range 45–92 years). We identified a 316 bp *Alu* insertion overlapping the *TMEM106B* 3′UTR tightly linked with top GWAS variants rs3173615(C) and rs1990622(A). In ADSP European ancestry participants, this insertion is in equivalent linkage with rs1990622(A) (R^2 = 0.962, D' = 0.998) and rs3173615(C) (R^2 = 0.960, D' = 0.996). In African ancestry participants, the insertion is in stronger linkage with rs1990622(A) (R^2 = 0.992, D' = 0.998) than with rs3173615(C) (R^2 = 0.811, D' = 0.994). In public data sets, rs1990622 was consistently associated with TMEM106B protein levels but not with mRNA expression. In the WUSTL data set, rs1990622 is associated with TMEM106B protein levels in plasma and CSF, but not with *TMEM106B* mRNA expression.

*These authors are cofirst authors and contributed equally.

†These authors are cosenior authors and contributed equally.

From the Department of Neurology and Neurological Sciences (A.C., Y.L.G., N.K., L.T., M.B., I.S., V.W.H., T.W.-C., M.D.G.); Quantitative Sciences Unit (Y.L.G.), Department of Medicine; Department of Genetics (Y.Z., J.G., T.D.J., A.D.G., E.A.); Division of Cardiology (J.G., E.A.), Department of Medicine, Stanford University School of Medicine, CA; Neurogenomics and Informatics Center (C.Y., C.C.), Washington University School of Medicine, St. Louis, MO; Wu Tsai Neurosciences Institute (A.D.W., E.M.); Department of Psychology (A.D.W., E.M.); and Department of Epidemiology and Population Health (V.W.H.), Stanford University, CA.

Go to Neurology.org/NG for full disclosures. Funding information is provided at the end of the article.

The Article Processing charge was funded by the authors.

Glossary

AD = Alzheimer disease; **ADRC** = Alzheimer Disease Research Center; **ADSP** = Alzheimer Disease Sequencing Project; **AF** = allele frequency; **eQTL** = expression quantitative trait locus; **FTLD-TDP** = frontotemporal lobar dementia with TDP-43 inclusions; **GWASs** = genome-wide association studies; **LD** = linkage disequilibrium; **LRS** = long-read sequencing; **NGS** = next-generation sequencing; **pQTL** = protein quantitative trait locus; **SAMS** = Stanford Aging and Memory Study; **SNVs** = single-nucleotide variants; **SVs** = structural variants; **USUHS** = Uniformed Services University of the Health Sciences; **WUSTL** = Washington University in St. Louis.

Discussion

We identified a novel *Alu* element insertion in the 3′UTR of *TMEM106B* in tight linkage with the lead FTLD-TDP risk variant. The lead variant is associated with TMEM106B protein levels, but not expression. The 3′UTR insertion is a lead candidate for the causal variant at this complex locus, pending confirmation with functional studies.

Introduction

Genome-wide association studies (GWASs) using imputed micro-array data or short-read next-generation sequencing (NGS) have identified single-nucleotide variants (SNVs) associated with neurodegenerative diseases. Variants associated with disease risk are frequently intergenic or intronic and rarely exonic. Among significant variants at a given locus, one may be causal or in linkage with a nearby genetic feature that is the true disease risk-modifying variant. Identifying the true causal variant at a GWAS locus is critical for elucidating disease pathogenesis and for developing candidate therapeutics. Structural variants (SVs)—which include large insertions, deletions, duplications, and other genomic features greater than 50 base pairs (bp) in length—are a source of genetic diversity whose effect on protein function is often readily interpretable because of their large size. SVs are challenging to identify with short-read NGS because of the typical 150 bp read length. SVs exceeding this length are detected in NGS data by analyzing paired and split-read evidence and changes in sequencing depth.[1-3] Emerging long-read sequencing (LRS) technology uses reads typically averaging 10–20 kilobases, enabling large SVs to be directly sequenced and correctly aligned to the genome.[4] LRS greatly enhances SV discovery over short-read NGS, identifying more than twice as many SVs as ensemble methods operating on short-read NGS data. Up to 83% of insertions identified by LRS are not detected by NGS algorithms.[5]

We performed LRS and SV calling for participants enrolled in Stanford's Iqbal Farrukh and Asad Jamal Alzheimer Disease Research Center (ADRC) and the Stanford Aging and Memory Study (SAMS).[6] We undertook an initial exploratory analysis looking for SVs overlapping exons, the 5′UTR or the 3′UTR of 4,579 genes linked in Gene Ontology to neurodegenerative disorders. This analysis revealed a 316 bp insertion on the 3′UTR of *TMEM106B* which—given the strong risk-modifying effects of a *TMEM106B* locus against frontotemporal lobar dementia with TAR DNA-binding protein pathology (frontotemporal lobar dementia with TDP-43 inclusions [FTLD-TDP])—we explored further.[7,8]

The initial FTLD-TDP GWAS[7] identified 3 significant SNVs (rs1990622, rs6966915, rs1020004) associated with reduced risk and in high linkage disequilibrium (LD) with one another, all on or near *TMEM106B*.[7] Subsequent work showed a pronounced effect on age-at-onset in *GRN* variant carriers with autosomal dominant FTLD-TDP.[9] The mechanism by which variants at the *TMEM106B* locus affect FTLD-TDP risk remains unclear because the significant variants are intronic or intergenic.[7] The only coding SNV in LD with rs1990622 is the missense variant rs3173615, which results in a p.T185S amino acid change in exon 6 of *TMEM106B*. A cell-based assay suggested that rs3173615 may hasten protein degradation.[10] However, an in vivo study using a $GRN^{-/-}$ mouse model homozygous for *TMEM106B**S186 (the conserved residue in mice) revealed no change in TMEM106B protein levels relative to wild type, nor amelioration of the pathologic lysosomal phenotype.[11] Furthermore, a meta-analysis of FTLD-TDP GWASs evaluating both rs1990622 and rs3173615 found that rs1990622 was the most significant SNV at the locus.[12] As such, the evidence for rs3173615 as the causative variant on *TMEM106B* remains mixed. Other studies have nominated an intergenic variant near rs1990622 that alters chromatin architecture and modulates *TMEM106B* expression[13] or 3′UTR variants that affect microRNA binding sites.[14] Recently, a large Alzheimer disease (AD) GWAS identified what appears to be the same *TMEM106B* locus. As in FTLD-TDP, the minor allele in European participants was associated with reduced risk for AD, although the effect size was much smaller. Given the uncertainty regarding the causal variant at this locus, we examined whether this newly identified *TMEM106B* 3′UTR insertion may mediate the observed effect on FTLD-TDP and AD risk.

Methods

Participants and Sources of Data

The Stanford ADRC is a cohort of healthy older controls and patients with AD and related neurologic disorders (n = 323 with LRS and short-read NGS, age range 45–92 years, 169 female and 154 male, healthy controls = 150, mild cognitive impairment individuals = 60, AD cases = 30, other diagnoses = 83). The SAMS is a cohort of cognitively unimpaired older individuals (n = 109 with LRS and short-read NGS, age range 60–88 years, 58 female and 51 male). The Washington University in St. Louis (WUSTL) participants were recruited as part of the Knight-ADRC and included longitudinally assessed community-dwelling adults enrolled by prospective studies of memory and aging (n = 1979 with short-read NGS, transcriptomics and/or CSF and/or plasma proteomics, age range 18–103 years, 1,034 female and 945 male, healthy controls = 1,005, AD cases = 858, other diagnoses = 116). The details on eligibility and assessments of participants in all data sets are provided in eMethods (links.lww.com/NXG/A670).

Long-Read Sequencing, Alignment, and SV Calling

High molecular weight DNA was extracted from primary blood mononuclear cells stored at −80C using a Puregene kit (Qiagen, Germany). DNA was sheared using a G-tube (Covaris LLC, MA). Sequencing libraries were prepared using Nanopore LSK-110 and sequenced on the PromethION48 (Oxford Nanopore Technologies, United Kingdom). An average of 50.4 gigabases were sequenced per sample, with a read length N50 of 18 kb. Sequencing data were base called using Guppy (High Accuracy, version 6.3) and aligned to hg38 using Minimap2.[15] Structural variants were called using Sniffles2[16] in population mode. SVs overlapping exons, the 5′UTR, or the 3′UTR of 4,579 genes linked in Gene Ontology to neurodegenerative disorders and extracted using the following keywords: ["neuro", "alzheimer", "apolipo", "amyloid"].

Short-Read Next-Generation Sequencing

TMEM106B SNV genotypes were determined from short-read NGS performed at either the Beijing Genomics Institute (BGI) in Shenzhen, China, on DNBseq platform (T10 and T7) or as part of the Stanford Extreme Phenotypes in Alzheimer Disease project with sequencing performed at the Uniformed Services University of the Health Sciences (USUHS) on an Illumina HiSeq platform. Among the 432 participants, 29 participants were sequenced at USUHS and 403 at BGI. The whole-genome targeted coverage for both platforms was 30x, and the read length was 150 bp. The Genome Analysis Toolkit (GATK) workflow germline short variant discovery was used to map genome sequencing data to the reference genome (hg38) and to produce high-confidence variant calls using joint calling.[17]

3′UTR Insertion and SNV Calls Validation With IGV

The genotypes of rs1990622, rs3173615, and the 3′UTR insertion were extracted for participants with both LRS and short-read NGS available. Eighteen individuals with discordant doses of the 3 variants in LRS—where the dose of any of the 3 variants differed from any other—were identified for validation with IGV. The manual validation protocol is described in eMethods (links.lww.com/NXG/A670).

Colocalization Analysis

Colocalization was performed using the R package *coloc*.[18] We report the posterior probability of colocalization (PP4) between AD[19] and FTLD-TDP.[7] Colocalization between the 2 GWAS results was visualized with *locuscompareR*.[20] Similarly, *coloc* analysis was performed between the plasma pQTL GWAS[21,22] and the 2 neurodegenerative diseases.[7,19]

ADSP Linkage Disequilibrium Analysis

Alzheimer disease sequencing project (ADSP) R.3 SNVs, Manta,[1] and Biograph[23] SV calls were downloaded from NIAGADS (dss.niagads.org/datasets/ng00067/#data-releases). SNVs were subset to rs3173615 (7:12229791:C:G) and rs1990622 (7:12244161:A:G) using Plink 1.9.[24] SNV genotyping and SV genotypes were available in 16,906 samples. After detailed curation of the SV genotypes (eMethods, links.lww.com/NXG/A670), 16,582 unique participants in ADSP had a robust calling of the 3′UTR insertion.

To identify European and African ancestry individuals in the ADSP, the ancestries of all ADSP individuals were determined using SNPWeights v2[25] with reference populations from the 1000 Genomes Consortium.[26] Individuals with greater than 75% African global ancestry were classified as African ancestry[27] and similarly for European ancestry.[28]

eQTL and pQTL Associations With the *TMEM106B* Locus

Expression quantitative trait locus (eQTL) and protein quantitative trait locus (pQTL) effect sizes and *p*-values were queried for rs1990622 from summary statistics (GTEx,[29] MetaBrain,[30] eQTLGen[31] for eQTLs and ARIC,[22] DECODE,[32] Wingo[33] for pQTLs).

In addition, we analyzed a novel data set collected at WUSTL, which included 1,979 participants with NGS (1,979 participants), blood bulk RNASeq (428 European participants, all healthy controls), plasma (1,150 European and 200 African participants, with 711 European and 120 African healthy controls), and CSF (1,210 European participants, with 588 healthy controls) proteomics obtained using SomaScan aptamers. Global ancestry was estimated using principal component analysis using the 1000 genome ancestry as anchors, and individuals were separated into European and African ancestry groups (eTable 1, links.lww.com/NXG/A670 provides the demographics by analyses). The details on the 'omics analysis methods are provided in eMethods. These

Figure 1 *TMEM106B* Locus Landscape and 3′ UTR Insertion Location

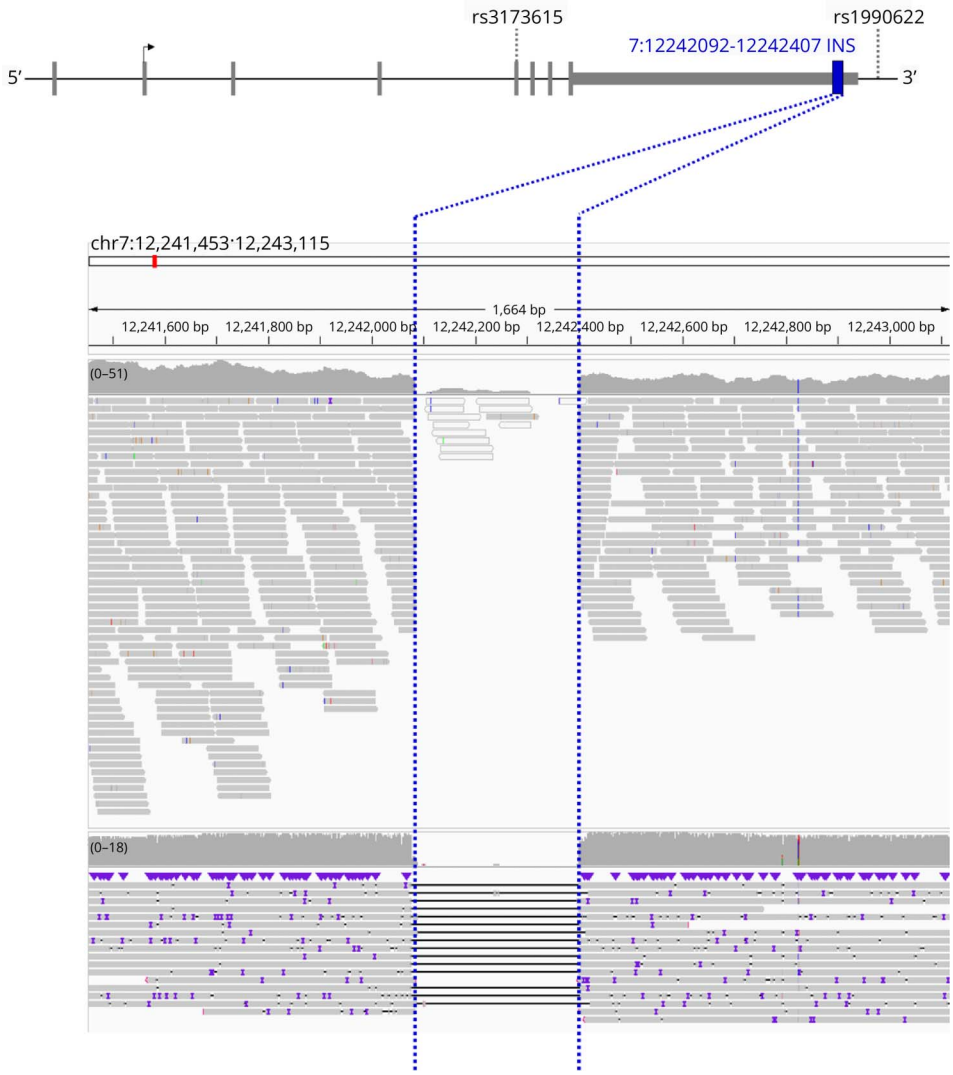

(Top) *TMEM106B* 3′ UTR insertion position relative to SNVs associated with FTLD-TDP. (Bottom) The *TMEM106B* 3′ UTR insertion, detected as a deletion compared with the reference genome, was seen in both next-generation sequencing (upper panel) and long-read sequencing (lower panel). The region corresponding to the structural variant is delineated with blue dotted lines. Both sequencing modalities are displayed here for a representative cohort participant without the *TMEM106B* 3′ UTR insertion. FTLD-TDP = frontotemporal lobar dementia with TDP-43 inclusions; SNVs = single nucleotide variants.

were adjusted for age and sex because of the association of TMEM106B and GRN protein levels with these 2 demographic factors (eFigures 1–3).

Standard Protocol Approvals, Registrations, and Patient Consents

Participants or their caregivers provided written informed consent in the original studies. Study protocols were approved by the Institutional Review Boards at Stanford University and WUSTL.

Data Availability

Data included in this study will be provided in an anonymized form on reasonable request made through email to the corresponding author and completion of a Material Transfer Agreement. See eAppendix 1 (links.lww.com/NXG/A670) for summary statistics data availability.

Results

We performed whole-genome LRS and SV calling for 432 participants enrolled in the Stanford ADRC or SAMS. In total, we identified 208 SVs overlapping an exon, 3′UTR, or 5′UTR site of one of the 4,579 genes considered. Among these, we identified a common 322 bp deletion on the 3′UTR of *TMEM106B* for further analysis given the interest in this locus (Figure 1A).[34] This SV overlaps a 316 bp *Alu*Yb8 mobile element that is prevalent in European ancestry individuals and is included in the hg38 reference genome.[35] Our analysis pipeline, therefore, detected this SV as a 322 bp deletion when comparing individual genomes to the hg38 reference. We will refer to the SV, hereafter, as an insertion.

The insertion is highly prevalent with allele frequency (AF) = 0.535 in our LRS data set, comparable with the major allele frequency, in European non-Finnish ancestry, in gnomAD

(v3.1.2) of rs1990622(A) (AF = 0.586) and rs3173615(C) (AF = 0.587). The insertion was detectable in both LRS and short-read NGS (Figure 1B). We linked LRS data to high coverage short-read NGS data to evaluate the LD between the 3′UTR insertion, rs1990622(A), and rs3173615(C). The *TMEM106B* 3′UTR insertion was in perfect LD with rs1990622(A) and rs3173615(C) in all but 2 Stanford individuals. For the sake of consistency, we will display all SNV data with the risk allele that is most often coinherited with the insertion. This is the A allele for rs1990622 and the C allele for rs3173615. Note that the insertion, rs1990722(A), and rs3173615(C) are the major alleles in European ancestry individuals (AF ~0.59) but the minor alleles in African ancestry individuals (AF ~0.27).

The linkage between the *TMEM106B* 3′UTR insertion, rs1990622(A), and rs3173615(C) was then established in a large cohort by querying the ADSP database. In total, 10,265 European ancestry and 2,212 African ancestry participants' samples were genotyped at both SNVs and the SV, with respective AFs for the *Alu* insertion of AF_{EUR} = 0.591 and AF_{AFR} = 0.272. In European ancestry individuals, the *Alu* insertion is in comparable LD with rs1990622 (R^2 = 0.962, D' = 0.998) and rs3173615 (R^2 = 0.960, D' = 0.996). In African ancestry individuals in ADSP, the *Alu* insertion is in stronger LD with rs1990622 (R^2 = 0.992, D' = 0.998) than with rs3173615 (R^2 = 0.811, D' = 0.994).

A colocalization analysis (Figure 2) demonstrated that the signals identified in the FTLD-TDP GWAS[7] and AD GWAS[19] at the *TMEM106B* locus have the same linkage structure (PP4 = 99.5%), suggesting that the same genetic signal is driving effects across both disorders.

We next evaluated the effect of rs1990622 on *TMEM106B* expression and protein levels in eQTL and pQTL data sets (Table). In a large brain eQTL data set (European ancestry-Metabrain; n = 6,601), rs1990622(A) was not associated with *TMEM106B* expression. In a smaller brain eQTL data set (African ancestry-Metabrain; n = 1,016), rs1990622(A) was significantly associated with increased *TMEM106B* expression. In 2 plasma eQTL data sets (GTEx, n = 670; and eQTLGen, n = 31,247), rs1990622(A) was significantly associated with decreased *TMEM106B* expression. In 3 large plasma pQTL data sets (deCODE; n = 35,371; ARIC European; n = 7,213; ARIC African; n = 1,871), rs1990622(A) was significantly associated with increased TMEM106B protein levels. In a smaller brain pQTL data set (Wingo; n = 722), rs1990622(A) was not significantly associated with TMEM106B protein levels (p = 0.1), but the direction of the effect was consistent with the plasma pQTL results. In addition, colocalization analyses showed that the plasma-based pQTL association with TMEM106B level in deCODE and ARIC colocalizes with the signal in AD and FTLD-TDP at the *TMEM106B* locus. Notably, all posterior probabilities of colocalization between the

Figure 2 Colocalization Between the AD[19] and FTLD-TDP[7] Genome-Wide Association Studies

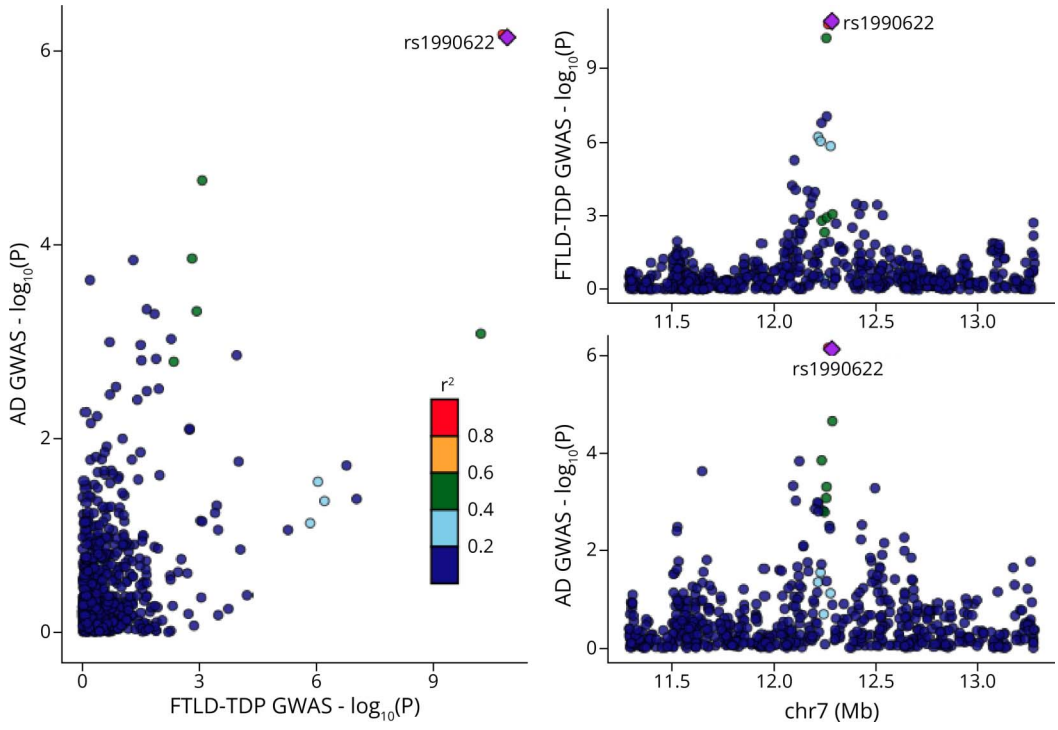

The posterior probability of colocalization (PP4) = 99.5%. Note that the FTLD-TDP GWASs only included directly genotyped variants, i.e., not imputed, and thus the intersection of the 2 GWASs on this 2 MB window is somewhat sparse, including only 607 variants. AD = Alzheimer disease; FTLD-TDP = frontotemporal lobar dementia with TDP-43 inclusions; GWASs = genome-wide association studies.

Table Effect of rs1990622 as a *TMEM106B* Expression Quantitative Trait Locus (eQTL) or Protein Quantitative Trait Locus (pQTL)

Data set	Tissue	Sample size	Effect size	*p* Value
Expression (e)QTL				
eQTLGen	Blood	31,427	-[a]	0.0174
GTEx	Blood	670	−0.25	4.00E-30
Metabrain EA	Brain (cortex)	6,601	+0.0268	0.3115
Metabrain AA	Brain (cortex)	1,016	+0.2053	0.0031
Protein (p)QTL				
deCODE	Plasma	35,371	+0.1106	3.69E-43
ARIC EA	Plasma	7,213	+0.2547	7.33E-53
ARIC AA	Plasma	1,871	+0.3147	1.50E-19
Wingo	Brain (cortex)	722	+0.0773	0.1005

Abbreviations: AA: African ancestry; EA: European ancestry.
All effect sizes are reported for the tested A allele with the G allele set as reference at rs1990622. Parameter estimates are those reported by respective studies and may be on different scales given different normalization procedures for transcriptomic and proteomic data.
[a] Negative Z-value indicating that A allele is associated with decreased *TMEM106B* expression.

densely imputed AD GWAS and TMEM106B protein level associations in plasma were above 80% (PP4 with deCODE = 81.1%; PP4 with ARIC European = 86.3%; PP4 with ARIC African = 91.6%) (eFigure 4, links.lww.com/NXG/A670).

To expand beyond these eQTL and pQTL results from publicly available databases, we tested the association between rs1990622 and *TMEM106B* expression, TMEM106B protein levels, and GRN protein levels in the WUSTL Neurogenomics data set.[36-38] First, we examined GRN and TMEM106B protein levels in a group of 11 carriers of FTLD-TDP–causing progranulin (*PGRN*) variants. The *PGRN* variant carriers have significantly higher plasma levels of TMEM106B compared with noncarriers from the same families ($p < 0.05$, Figure 3A). GRN levels were significantly lower in *PRGN* variant carriers compared with noncarriers from the same families ($p < 0.001$, Figure 3B). With only 11 *PGRN* variant carriers, we could not determine whether the *TMEM106B* locus variants affected TMEM106B or GRN levels. When comparing AD cases vs older controls, we found that plasma TMEM106B levels were significantly lower in AD ($\beta = -0.011$; 95% CI [−0.019 to −0.004]; $p = 4.25 \times 10^{-3}$) as were CSF TMEM106B levels ($\beta = -0.186$; 95% CI [−0.277 to −0.095]; $p = 6.35 \times 10^{-5}$). We also found a significant increase in plasma ($\beta = 0.016$; 95% CI [0.002; 0.031]; $p = 0.021$) and

Figure 3 Differential Abundance Analysis of PGRN Variant Carriers vs Noncarriers on Plasma TMEM106B and GRN Protein Levels

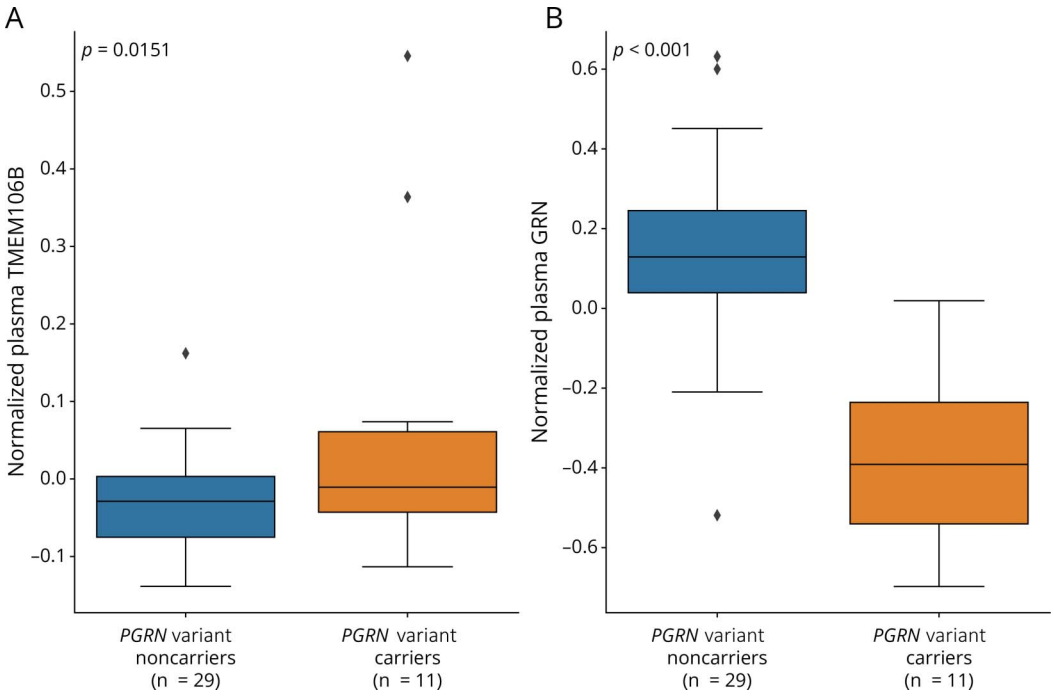

(A) Boxplot of the normalized plasma protein *TMEM106B* levels between *PGRN* variant carriers and noncarriers. Variant carriers have significantly higher TMEM106B levels ($p = 0.0151$). (B) Boxplot of normalized plasma protein *GRN* levels between *PGRN* variant carriers and noncarriers. Variant carriers have significantly lower GRN levels ($p = 2.89 \times 10^{-8}$). Analyses were adjusted for age, sex, and proteomic principal components 1 and 2.

CSF GRN levels (β = 0.0969; 95% CI [0.004–0.19]; $p = 0.04$) when comparing AD cases with controls.

In the large WUSTL cohort of healthy older European ancestry controls, rs1990622 was not associated with *TMEM106B* expression levels ($p = 0.87$) in blood but was associated with TMEM106B protein levels in both plasma and CSF (Figure 4). rs1990622(A) was significantly associated with increased levels of TMEM106B in plasma (β = 0.0227; 95% CI [0.015–0.031]; $p = 5.6 \times 10^{-8}$) and in CSF (β = 0.280; 95% CI [0.232–0.327]; $p = 3.9 \times 10^{-27}$), with a roughly 10-fold larger effect size in CSF. rs1990622(A) was also associated with TMEM106B protein levels in plasma of African ancestry controls (β = 0.0290; 95% CI [0.002–0.057]; $p = 0.0387$ and eTable 2, links.lww.com/NXG/A670). There were not enough African ancestry CSF samples to perform similar analyses. In examining GRN levels, we did not find a significant association of rs1990622(A) with GRN levels in plasma or CSF.

Because rs1990622 and rs3173615 were called directly from NGS in the WUSTL data, we could compare the effect sizes of the 2 SNVs directly. The results were nearly identical with a numerically larger effect of rs1990622 in plasma and CSF of European ancestry participants and a numerically larger effect of rs3173615 in plasma of African ancestry participants (eTable 2, eFigure 5, links.lww.com/NXG/A670).

Discussion

The *TMEM106B* 3′UTR *Alu*Yb8 insertion is a previously unreported variant that may mediate the effect of the *TMEM106B* locus on FTLD-TDP risk and AD risk. At present, the candidates for the causal variant at this locus are (1) the *TMEM106B* 3′UTR insertion described here; (2) rs3173615, the only coding SNV in this linkage block; (3) rs1990622, the leading GWAS hit; or (4) another variant in this linkage block.

Here, we used publicly available expression and protein data sets to establish that rs1990622 is a consistent pQTL but an inconsistent eQTL and then confirmed this in a large, novel transcriptomics and proteomics data set from WUSTL. This suggests that the effect at the *TMEM106B* locus is likely mediated by a genetic variant that acts after transcription to impact TMEM106B protein levels. Because intronic and intergenic variants are not incorporated into the processed mRNA molecule, it is less likely that such variants, including rs1990622, are directly mediating the effect of this locus. Furthermore, the pQTL findings, coupled with the finding of increased TMEM106B protein levels in *PGRN* variant carriers, suggest that the *TMEM106B* locus exerts its effect by altering protein availability rather than by altering protein function because of an amino acid change. This reduces the likelihood that rs3173615 is the causal variant. A previous in vitro study suggested that the TMEM106B *p*.S185 protein is less stable than wild type and may, therefore, result in reduced protein levels,[10] but recent in vivo mouse model work suggests that the rs3173615 missense variant is not causal.[11] Moreover, rs1990622 was found to be more significant than rs3173615 in an FTLD-TDP GWAS meta-analysis,[12] which would be unexpected if the protective effect of the rs1990622 minor allele were due to its linkage with rs3173615.

Figure 4 Effects of rs1990622 on *TMEM106B* Gene Expression in Blood and TMEM106B Protein Levels in Plasma and CSF of European Ancestry Controls

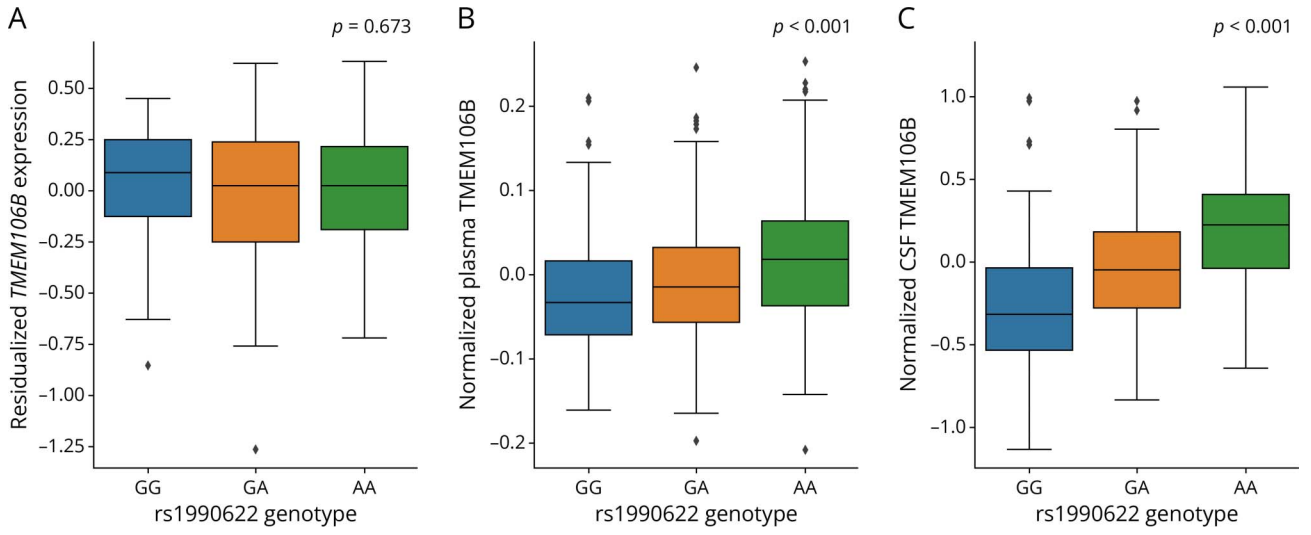

(A) Boxplot of the residualized *TMEM106B* gene expression in healthy older control blood samples across the rs1990622 genotypes (beta = 0.00481, $p = 0.673$). (B) Boxplot of normalized TMEM106B protein levels from plasma in healthy older controls across the rs1990622 genotypes (beta = 0.0215, $p = 6.3 \times 10^{-11}$). (C) Boxplot of normalized TMEM106B protein levels from CSF in healthy older controls across the rs1990622 genotypes (beta = 0.283, $p = 2.5 \times 10^{-32}$). All analyses were adjusted for age and sex.

We found in ADSP that the *TMEM106B* 3′UTR insertion is in higher LD with rs1990622(A) than rs3173615(C), which is consistent with a model in which the respective significance of these 2 SNVs is related to their linkage with the *TMEM106B* 3′UTR insertion. The proteomics data from WUSTL showed that the effect sizes of these variants are almost identical for CSF and plasma TMEM106B levels with a minimally larger effect for rs1990622 in European ancestry participants and a minimally larger effect for rs3173615 in African ancestry individuals. We emphasize here that the differences between the 2 variants on protein levels are exceedingly small and should not be considered significant. Directly comparing the effect size of the 2 SNVs in the same set of participants would be more powerful in a large sample of African ancestry AD cases and controls or a larger sample of African ancestry proteomics data set given that roughly 6% of African ancestry haplotypes are discordant across these 2 SNVs compared with only ~0.5% of European ancestry haplotypes. With the growing focus on enrolling more underrepresented minority participants in genetics studies, such an analysis should be feasible in the near future. Given the high LD across the locus, such analyses will be more reliable and definitive when carried out on short-read NGS or LRS data sets rather than on imputed SNV array data sets.

There are several possibilities as to how the *TMEM106B* 3′UTR *Alu* insertion could increase risk in FTLD-TDP and AD. The pQTL evidence indicates that the major risk allele at the *TMEM106B* locus increases TMEM106B protein levels both in plasma and in CSF. In the cortex, the trend is in the same direction but did not reach significance ($p = 0.10$) with this relatively smaller sample size (Table). In a small group of *PGRN* variant carriers, we replicate previous work[9,39,40] showing reduced plasma levels of GRN and demonstrate, for the first time, that TMEM106B levels are increased. As FTLD-TDP due to *PGRN* variants is thought to result from haploinsufficiency of GRN,[34,41,42] a compelling hypothesis is that the *Alu* insertion on the 3′UTR results in an increase of TMEM106B levels in the brain which further depletes GRN levels. These 2 proteins are both major components of the endolysosomal pathway and so are well-positioned to interact[37,43] Further evidence that the 2 proteins interact comes from recent work demonstrating that TMEM106B fibrils form aggregates in a variety of neurodegenerative disorders and as a function of age, but that these TMEM106B fibrils are far more prominent in *PGRN* variant carriers with FTLD-TDP.[44-47] In AD, we found the opposite pattern (reduced TMEM106B levels and increased GRN levels in plasma and in CSF). This is less readily interpretable given that we do not understand GRN's role in AD. One possibility is that the findings in AD reflect compensatory changes in the setting of pathogenesis rather than causal effects driving pathogenesis.

The mechanism by which the insertion may affect TMEM106B levels remains uncertain. The insertion may result in selective enrichment of an alternate transcript polyadenylation site, changing the 3′UTR. Such a change in the 3′UTR could affect protein binding, which may in turn affect translational efficiency, alter the subcellular localization of the RNA, or impair protein routing to the endoplasmic reticulum.[48] Identifying a clear-cut mechanism linking the insertion to increased TMEM106B protein levels is still required to confirm that this is the causal variant at the locus.

In summary, we report a 316 bp *Alu* insertion on *TMEM106B* that is in tight LD with rs1990622(A) and rs3173615(C) in a large LRS data set. LRS provides a valuable tool for the detection of large genomic variants that can aid in the interpretation of GWAS results and elucidate genetic drivers of the disease. Ongoing functional work by our group and others will elaborate on the mechanisms connecting the 3′UTR *Alu*Yb8 insertion to pathogenesis in FTLD-TDP and AD.

Acknowledgment

Acknowledgements are included in eAppendix 2 (links.lww.com/NXG/A670).

Study Funding

This work was supported by the following NIH grants to Stanford investigators: RO1AG060747; R35AG072290; R01AG048076; R01AG074339; P30AG066515; and K99AG075238. This work was also supported by the Alzheimer's Association (AARF-20-683984). Multiomics data generated by the NeuroGenomics and Informatics Funding was supported by grants from the NIH: R01AG044546; P01AG003991; RF1AG053303: RF1AG058501; U01AG058922;, RF1AG074007; the Chan Zuckerberg Initiative (CZI); the Michael J. Fox Foundation; the Department of Defense (W81XWH2010849); the Alzheimer's Association Zenith Fellows Award (ZEN-22-848604); and an Anonymous foundation. The recruitment and clinical characterization of research participants at Washington University were supported by NIH P30AG066444; P01AG03991; and P01AG026276. This work was supported by access to equipment made possible by the Hope Center for Neurological Disorders, the Neurogenomics and Informatics Center (NGI: neurogenomics.wustl.edu/), and the Departments of Neurology and Psychiatry at Washington University School of Medicine. The following investigators assisted in the preparation of the WUSTL 'omics data set Matt Johnson, Maulikkumar Patel, Maria Victoria Fernandez, Jessie Sanford, Devin Dikec, Ellen Liu, Dan Western, Thomas Marsh, Priyanka Gorijala, Jigyasha Timsina, and Judy Lihua Wang.

Disclosure

The authors report no relevant disclosures. Go to Neurology.org/NG for full disclosures.

Publication History

Received by *Neurology: Genetics* November 6, 2023. Accepted in final form November 27, 2023. Submitted and externally peer reviewed. The handling editor was Editor Stefan M. Pulst, MD, Dr med, FAAN.

Appendix Authors

Name	Location	Contribution
Augustine Chemparathy, MS	Department of Neurology and Neurological Sciences, Stanford University School of Medicine, CA	Drafting/revision of the manuscript for content, including medical writing for content; major role in the acquisition of data; study concept or design; analysis or interpretation of data
Yann Le Guen, PhD	Department of Neurology and Neurological Sciences; Quantitative Sciences Unit, Department of Medicine, Stanford University School of Medicine, CA	Drafting/revision of the manuscript for content, including medical writing for content; major role in the acquisition of data; study concept or design; analysis or interpretation of data
Yi Zeng, PhD	Department of Genetics, Stanford University School of Medicine, CA	Study concept or design; analysis or interpretation of data
John Gorzynski, DVM, PhD	Department of Genetics; Division of Cardiology, Department of Medicine, Stanford University School of Medicine, CA	Drafting/revision of the manuscript for content, including medical writing for content; major role in the acquisition of data; study concept or design; analysis or interpretation of data
Tanner D. Jensen, BS	Department of Genetics, Stanford University School of Medicine, CA	Drafting/revision of the manuscript for content, including medical writing for content; major role in the acquisition of data; study concept or design; analysis or interpretation of data
Chengran Yang, PhD	Neurogenomics and Informatics Center, Washington University School of Medicine, St. Louis, MO	Drafting/revision of the manuscript for content, including medical writing for content; major role in the acquisition of data; study concept or design; analysis or interpretation of data
Nandita Kasireddy, BA	Department of Neurology and Neurological Sciences, Stanford University School of Medicine, CA	Drafting/revision of the manuscript for content, including medical writing for content; major role in the acquisition of data; study concept or design; analysis or interpretation of data
Lia Talozzi, PhD	Department of Neurology and Neurological Sciences, Stanford University School of Medicine, CA	Major role in the acquisition of data; study concept or design; analysis or interpretation of data
Michael Belloy, PhD	Department of Neurology and Neurological Sciences, Stanford University School of Medicine, CA	Major role in the acquisition of data; study concept or design; analysis or interpretation of data
Ilaria Stewart, BA	Department of Neurology and Neurological Sciences, Stanford University School of Medicine, CA	Drafting/revision of the manuscript for content, including medical writing for content; major role in the acquisition of data; study concept or design; analysis or interpretation of data

Appendix *(continued)*

Name	Location	Contribution
Aaron D. Gitler, PhD	Department of Genetics, Stanford University School of Medicine, CA	Study concept or design; analysis or interpretation of data
Anthony D. Wagner, PhD	Wu Tsai Neurosciences Institute; Department of Psychology, Stanford University, Stanford, CA	Study concept or design; analysis or interpretation of data
Elizabeth Mormino, PhD	Wu Tsai Neurosciences Institute; Department of Psychology, Stanford University, Stanford, CA	Study concept or design; analysis or interpretation of data
Victor W. Henderson, MD, MS	Department of Neurology and Neurological Sciences, Stanford University School of Medicine; Department of Epidemiology and Population Health, Stanford University, CA	Study concept or design; analysis or interpretation of data
Tony Wyss-Coray, PhD	Department of Neurology and Neurological Sciences, Stanford University School of Medicine, CA	Study concept or design; analysis or interpretation of data
Euan Ashley, MB, ChB, DPhil	Department of Genetics; Division of Cardiology, Department of Medicine, Stanford University School of Medicine, CA	Major role in the acquisition of data; study concept or design; analysis or interpretation of data
Carlos Cruchaga, PhD	Neurogenomics and Informatics Center, Washington University School of Medicine, St. Louis, MO	Drafting/revision of the manuscript for content, including medical writing for content; major role in the acquisition of data; study concept or design; analysis or interpretation of data
Michael D. Greicius, MD, MPH	Department of Neurology and Neurological Sciences, Stanford University School of Medicine, CA	Drafting/revision of the manuscript for content, including medical writing for content; major role in the acquisition of data; study concept or design; analysis or interpretation of data

References

1. Chen X, Schulz-Trieglaff O, Shaw R, et al. Manta: rapid detection of structural variants and indels for germline and cancer sequencing applications. *Bioinformatics*. 2016; 32(8):1220-1222. doi:10.1093/bioinformatics/btv710
2. Pedersen BS, Quinlan AR. Duphold: scalable, depth-based annotation and curation of high-confidence structural variant calls. *Gigascience*. 2019;8(4):giz040. doi:10.1093/gigascience/giz040
3. Mahmoud M, Gobet N, Cruz-Dávalos DI, Mounier N, Dessimoz C, Sedlazeck FJ. Structural variant calling: the long and the short of it. *Genome Biol.* 2019;20(1):246. doi:10.1186/s13059-019-1828-7
4. Logsdon GA, Vollger MR, Eichler EE. Long-read human genome sequencing and its applications. *Nat Rev Genet.* 2020;21(10):597-614. doi:10.1038/s41576-020-0236-x
5. Chaisson MJP, Sanders AD, Zhao X, et al. Multi-platform discovery of haplotype-resolved structural variation in human genomes. *Nat Commun.* 2019;10(1):1784. doi:10.1038/s41467-018-08148-z
6. Trelle AN, Carr VA, Guerin SA, et al. Hippocampal and cortical mechanisms at retrieval explain variability in episodic remembering in older adults. *Elife*. 2020;9: e55335. doi:10.7554/eLife.55335
7. Van Deerlin VM, Sleiman PMA, Martinez-Lage M, et al. Common variants at 7p21 are associated with frontotemporal lobar degeneration with TDP-43 inclusions. *Nat Genet* 2010;42(3):234-239. doi:10.1038/ng.536
8. Li Z, Farias FHG, Dube U, et al. The TMEM106B FTLD-protective variant, rs1990621, is also associated with increased neuronal proportion. *Acta Neuropathol.* 2020;139(1):45-61. doi:10.1007/s00401-019-02066-0

9. Cruchaga C, Graff C, Chiang HH, et al. Association of TMEM106B gene polymorphism with age at onset in granulin mutation carriers and plasma granulin protein levels. *Arch Neurol.* 2011;68(5):581-586. doi:10.1001/archneurol.2010.350
10. Nicholson AM, Finch NA, Wojtas A, et al. TMEM106B p.T185S regulates TMEM106B protein levels: implications for frontotemporal dementia. *J Neurochem.* 2013;126(6):781-791. doi:10.1111/jnc.12329
11. Cabron AS, Borgmeyer U, Richter J, et al. Lack of a protective effect of the Tmem106b "protective SNP" in the Grn knockout mouse model for frontotemporal lobar degeneration. *Acta Neuropathol Commun.* 2023;11(1):21. doi:10.1186/s40478-023-01510-3
12. Pottier C, Zhou X, Perkerson RB 3rd, et al. Potential genetic modifiers of disease risk and age at onset in patients with frontotemporal lobar degeneration and GRN mutations: a genome-wide association study. *Lancet Neurol.* 2018;17(6):548-558. doi:10.1016/S1474-4422(18)30126-1
13. Gallagher MD, Posavi M, Huang P, et al. A dementia-associated risk variant near TMEM106B alters chromatin architecture and gene expression. *Am J Hum Genet.* 2017;101(5):643-663. doi:10.1016/j.ajhg.2017.09.004
14. Chen-Plotkin AS, Unger TL, Gallagher MD, et al. TMEM106B, the risk gene for frontotemporal dementia, is regulated by the microRNA-132/212 cluster and affects progranulin pathways. *J Neurosci.* 2012;32(33):11213-11227. doi:10.1523/JNEUROSCI.0521-12.2012
15. Li H. Minimap2: pairwise alignment for nucleotide sequences. *Bioinformatics.* 2018;34(18):3094-3100. doi:10.1093/bioinformatics/bty191
16. Smolka M, Paulin LF, Grochowski CM, et al. Detection of mosaic and population-level structural variants with Sniffles2. *Nature Biotechnology.* Published online January 2, 2024. doi:10.1038/s41587-023-02024-y
17. Poplin R, Ruano-Rubio V, DePristo MA, et al. Scaling accurate genetic variant discovery to tens of thousands of samples. *bioRxiv*. Published online July 24, 2018. doi:10.1101/201178
18. Giambartolomei C, Vukcevic D, Schadt EE, et al. Bayesian test for colocalisation between pairs of genetic association studies using summary statistics. *PLoS Genet.* 2014;10(5):e1004383. doi:10.1371/journal.pgen.1004383
19. Bellenguez C, Küçükali F, Jansen IE, et al. New insights into the genetic etiology of Alzheimer's disease and related dementias. *Nat Genet.* 2022;54(4):412-436. doi:10.1038/s41588-022-01024-z
20. Liu B, Gloudemans MJ, Rao AS, Ingelsson E, Montgomery SB. Abundant associations with gene expression complicate GWAS follow-up. *Nat Genet.* 2019;51(5):768-769. doi:10.1038/s41588-019-0404-0
21. Beyter D, Ingimundardottir H, Oddsson A, et al. Long-read sequencing of 3,622 Icelanders provides insight into the role of structural variants in human diseases and other traits. *Nat Genet.* 2021;53(6):779-786. doi:10.1038/s41588-021-00865-4
22. Zhang J, Dutta D, Köttgen A, et al. Plasma proteome analyses in individuals of European and African ancestry identify cis-pQTLs and models for proteome-wide association studies. *Nat Genet.* 2022;54(5):593-602. doi:10.1038/s41588-022-01051-w
23. English AC, McCarthy N, Flickenger R, et al. Leveraging a WGS compression and indexing format with dynamic graph references to call structural variants. *bioRxiv*. Published online April 25, 2020. doi:10.1101/2020.04.24.060202
24. Chang CC, Chow CC, Tellier LC, Vattikuti S, Purcell SM, Lee JJ. Second-generation PLINK: rising to the challenge of larger and richer datasets. *Gigascience.* 2015;4:7. doi:10.1186/s13742-015-0047-8
25. Chen CY, Pollack S, Hunter DJ, Hirschhorn JN, Kraft P, Price AL. Improved ancestry inference using weights from external reference panels. *Bioinformatics.* 2013;29(11):1399-1406. doi:10.1093/bioinformatics/btt144
26. 1000 Genomes Project Consortium, Auton A, Brooks LD, et al. A global reference for human genetic variation. *Nature.* 2015;526(7571):68-74. doi:10.1038/nature15393
27. Le Guen Y, Raulin AC, Logue MW, et al. Association of African ancestry-specific APOE missense variant R145C with risk of Alzheimer disease. *JAMA.* 2023;329(7):551-560. doi:10.1001/jama.2023.0268
28. Le Guen Y, Belloy ME, Grenier-Boley B, et al. Association of rare APOE missense variants V236E and R251G with risk of Alzheimer disease. *JAMA Neurol.* 2022;79(7):652-663. doi:10.1001/jamaneurol.2022.1166
29. GTEx Consortium. The GTEx Consortium atlas of genetic regulatory effects across human tissues. *Science.* 2020;369(6509):1318-1330. doi:10.1126/science.aaz1776
30. de Klein N, Tsai EA, Vochteloo M, et al. Brain expression quantitative trait locus and network analyses reveal downstream effects and putative drivers for brain-related diseases. *Nat Genet.* 2023;55(3):377-388. doi:10.1038/s41588-023-01300-6
31. Võsa U, Claringbould A, Westra HJ, et al. Large-scale cis- and trans-eQTL analyses identify thousands of genetic loci and polygenic scores that regulate blood gene expression. *Nat Genet.* 2021;53(9):1300-1310. doi:10.1038/s41588-021-00913-z
32. Beyter D, Ingimundardottir H, Oddsson A, et al. Long read sequencing of 3,622 Icelanders provides insight into the role of structural variants in human diseases and other traits. *bioRxiv*. 2020:848366. doi:10.1101/848366
33. Wingo T, Liu Y, Gerasimov ES, et al. Integrating human brain proteomes with GWAS results to identify causal brain proteins for the major psychiatric disorders. *Biol Psychiatry*. 2023;93(9):S55-S56. doi:10.1016/j.biopsych.2023.02.153
34. Chemparathy A, Le Guen Y, Zeng Y, et al. A 3'UTR insertion is a candidate causal variant at the *TMEM106B* locus associated with increased risk for FTLD-TDP. *medRxiv*. Published online July 8, 2023. doi:10.1101/2023.07.06.23292312
35. Salazar A, Tesi N, Hulsman M, et al. An AluYb8 mobile element further characterises a risk haplotype of TMEM106B associated in neurodegeneration. *bioRxiv*. Published online July 16, 2023. doi: 10.1101/2023.07.16.23292721
36. Wang C, Western D, Yang C, et al. Unique genetic architecture of CSF and brain metabolites pinpoints the novel targets for the traits of human wellness. *Res Sq*. Published online June 9, 2023. doi:10.21203/rs.3.rs-2923409/v1
37. Cruchaga C, Western D, Timsina J, et al. Proteogenomic analysis of human cerebrospinal fluid identifies neurologically relevant regulation and informs causal proteins for Alzheimer's disease. *Res Sq*. Published online June 9, 2023. doi:10.21203/rs.3.rs-2814616/v1
38. Phillips B, Western D, Wang L, et al. Proteome wide association studies of LRRK2 variants identify novel causal and druggable proteins for Parkinson's disease. *NPJ Parkinsons Dis.* 2023;9(1):107. doi:10.1038/s41531-023-00555-4
39. Finch N, Baker M, Crook R, et al. Plasma progranulin levels predict progranulin mutation status in frontotemporal dementia patients and asymptomatic family members. *Brain*. 2009;132(Pt 3):583-591. doi:10.1093/brain/awn352
40. Meeter LHH, Patzke H, Loewen G, et al. Progranulin levels in plasma and cerebrospinal fluid in granulin mutation carriers. *Dement Geriatr Cogn Dis Extra.* 2016;6(2):330-340. doi:10.1159/000447738
41. Baker M, Mackenzie IR, Pickering-Brown SM, et al. Mutations in progranulin cause tau-negative frontotemporal dementia linked to chromosome 17. *Nature*. 2006;442(7105):916-919. doi:10.1038/nature05016
42. Gass J, Cannon A, Mackenzie IR, et al. Mutations in progranulin are a major cause of ubiquitin-positive frontotemporal lobar degeneration. *Hum Mol Genet* 2006;15(20):2988-3001. doi:10.1093/hmg/ddl241
43. Brady OA, Zheng Y, Murphy K, Huang M, Hu F. The frontotemporal lobar degeneration risk factor, TMEM106B, regulates lysosomal morphology and function. *Hum Mol Genet.* 2013;22(4):685-695. doi:10.1093/hmg/dds475
44. Jiang YX, Cao Q, Sawaya MR, et al. Amyloid fibrils in FTLD-TDP are composed of TMEM106B and not TDP-43. *Nature*. 2022;605(7909):304-309. doi:10.1038/s41586-022-04670-9
45. Chang A, Xiang X, Wang J, et al. Homotypic fibrillization of TMEM106B across diverse neurodegenerative diseases. *Cell.* 2022;185(8):1346-1355.e15. doi:10.1016/j.cell.2022.02.026
46. Schweighauser M, Arseni D, Bacioglu M, et al. Age-dependent formation of TMEM106B amyloid filaments in human brains. *Nature*. 2022;605(7909):310-314. doi:10.1038/s41586-022-04650-z
47. Perneel J, Neumann M, Heeman B, et al. Accumulation of TMEM106B C-terminal fragments in neurodegenerative disease and aging. *Acta Neuropathol.* 2023;145(3):285-302. doi:10.1007/s00401-022-02531-3
48. Mitschka S, Mayr C. Context-specific regulation and function of mRNA alternative polyadenylation. *Nat Rev Mol Cell Biol.* 2022;23(12):779-796. doi:10.1038/s41580-022-00507-5